

Article

# Power Control Method for Energy Efficient Buffer-Aided Relay Systems

Jingon Joung <sup>1</sup>, Han Lim Lee <sup>1</sup>, Jian Zhao <sup>2</sup> and Xin Kang <sup>3,\*</sup><sup>1</sup> School of Electrical and Electronics Engineering, Chung-Ang University, Seoul 06974, Korea<sup>2</sup> School of Electronic Science and Engineering, Nanjing University, Nanjing 210023, China<sup>3</sup> Center for Intelligent Networking and Communications (CINC), University of Electronic Science and Technology of China (UESTC), Chengdu 611731, China

\* Correspondence: kangxin@uestc.edu.cn; Tel.: +82-2-820-5145

Received: 2 June 2019; Accepted: 20 August 2019; Published: 22 August 2019



**Abstract:** In this paper, a power control method is proposed for a buffer-aided relay node (RN) to enhance the energy efficiency of the RN system. By virtue of a buffer, the RN can reserve the data at the buffer when the the channel gain between an RN and a destination node (DN) is weaker than that between SN and RN. The RN then opportunistically forward the reserved data in the buffer according to channel condition between the RN and the DN. By exploiting the buffer, RN reduces transmit power when it reduces the transmit data rate and reserve the data in the buffer. Therefore, without any total throughput reduction, the power consumption of RN can be reduced, resulting in the energy efficiency (EE) improvement of the RN system. Furthermore, for the power control, we devise a simple power control method based on a two-dimensional surface fitting model of an optimal transmit power of RN. The proposed RN power control method is readily and locally implementable at the RN, and it can significantly improve EE of the RN compared to the fixed power control method and the spectral efficiency based method as verified by the rigorous numerical results.

**Keywords:** UAV; relay; cooperative communications; buffer; power control; energy efficiency

## 1. Introduction

Initiated by the information theoretical perspective research on the cooperative communications using a relay node (RN) [1–5], various cooperative communication techniques have been studied to improve communication reliability, such as spectral efficiency (SE) and bit-error-rate (BER), and/or enlarge the coverage of the communications [6,7]. For example, in works by the authors of [2,3], SE was considered as a key performance metric of the cooperative networks, and in the work by the authors of [4], source precoder, relaying matrices, and destination decoder were iteratively optimized to improve BER performance. There are various retransmission strategies and duplex methods for the relaying. Amplify-and-forward (AF) relays simply amplify and forward (retransmit) the received signal [8–12], while decode-and-forward (DF) relays decode, encode, and forward the signal under certain conditions [2,13]. Full-duplex (FD) relay can transmit and receive the signal simultaneously, while a half-duplex (HD) relay receives and transmits separately [2].

Recently, unmanned aerial vehicles (UAV) have been rigorously studied as RN or base station (BS) [14–17]. If the UAV is employed as a relay, i.e., RN, it can forward the ground BS signals to other UAVs in the air. Here, a highly limited resource, i.e., energy, should be carefully managed to prolong the battery life of the RN. To this end, energy efficiency (EE) of the cooperative system has to be emphasized in resource management. For example, in the work by the authors of [18], a resource allocation strategy including power allocation was studied for a relay system to enhance the EE of the cooperative system. In the work by the authors of [19], a near-optimal iterative subcarrier pairing

algorithm and power allocation was proposed to improve EE of DF relay networks. For a mobile RN, SE and EE are considered [20].

Based on the observation that the same achievable rate can be achieved with lower transmit power of the RN compared to an RN without the buffer, it was shown that the achievable rate can be increased by employing a buffer at the RN (see works by the authors of [21–24] and the references therein). In the work by the authors of [24], the frequency and power resources were optimally allocated for multiple nodes to improve the EE of the buffer-aided relay networks. Adapting the buffer at RN allows the opportunistic retransmission, and the average achievable rate performance can thus be improved. Moreover, the packet delay and outage probability can also be reduced by using the buffer [25].

In this study, the EE of a buffer-aided fixed RN system is investigated under the assumption that the transmit power of the source node (SN) is also fixed. Here, we assume that SN and HD-DF RN are located at the fixed positions as shown in Figure 1. The RN serves the SN and destination node (DN) as a signal repeater that forwards the received signals from the SN to DN. This scenario is similar to the conventional cellular communication scenario using a repeater that forwards the outdoor base station (i.e., SN) signals to an indoor mobile user (i.e., DN) in a building [26]. Thus, the assumption of the fixed SN and RN are reasonable and many of studies regarding the cooperative communications has been performed for the fixed RN [27–30]. For the buffer-aided fixed RN, we propose a method to control the transmit power of RN based on the RN power consumption model and the distance between RN and DN to improve the network EE. The achievable rate is derived, and using it and an RN power consumption model, the EE of the network is formulated. Since it is intractable to derive the derivative of the EE function with respect to the transmit power and EE is a function of various power consumption parameters, analytical design of the optimal power control strategy is formidable. Since analytical optimization methods, e.g., the resource allocation method in the work by the authors of [24], require the channel state information among the nodes at the transmitter, the practical implementation is challenging. Even any conventional one-dimensional numerical search algorithm or a learning-based method, e.g., a reinforcement learning, is not applicable as it requires the achievable rate at DN at each iteration. This causes a significant network overhead as the achievable rate information or channel state information is needed to be fed back from DN to RN. Therefore, we devise a simple power control method based on a model of the optimal transmit power of RN. To model the optimal transmit power of RN, we extract two essential parameters that determine the transmit power of RN: (i) constant power consumption  $P_c$  at RN and (ii) distance  $d_{rd}$  between RN and DN. The optimal transmit power of RN are then modeled with respect to  $P_c$  and  $d_{rd}$  by using a two-dimensional surface fitting method. For the RN power control, thus, only  $P_c$  and  $d_{rd}$  information is required at RN. Here,  $P_c$  is local information, which can be readily measured at RN. The distance  $d_{rd}$  can also be measured at RN based on the received signal strength from DN. Therefore, the proposed RN power control method is easily implementable at the RN. From the rigorous numerical results, it is verified that the proposed power control method can significantly improve EE compared to the fixed power control method regardless of  $P_c$  and  $d_{rd}$ .

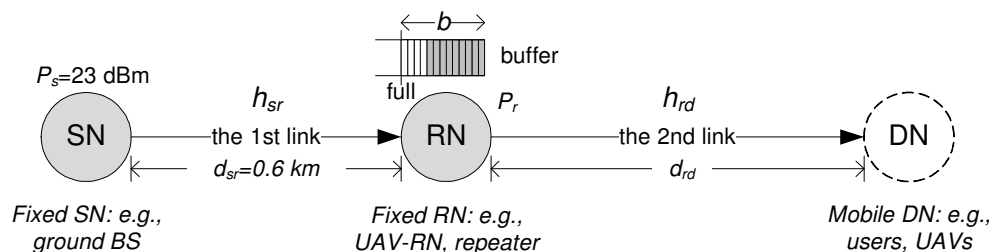


**Figure 1.** Buffer-aided relay system model, where  $P_s$  and  $P_r$  are the transmit power of the source node (SN) and relay node (RN), respectively;  $d_{sr}$  and  $d_{rd}$  are the distance between SN and RN and between RN and DN, respectively; and  $b$  is the size of the buffer.

## 2. RN System Model

Consider an RN system as shown in Figure 1, in which SN transmits data to DN through RN. RN is located at the fixed position  $d_{sr}$  km apart from SN. Each node has a single antenna. DN could be either an UAV in the air or ground user, whose direct link to SN is blocked due to the obstacles between SN and DN. The channel of the first link between SN and RN is denoted by  $h_{sr} = \sqrt{\rho_{sr}}\bar{h}_{sr}$ . Here,  $\rho_{sr}$  is the large-scale fading between SN and RN, and small-scale fading  $\bar{h}_{sr}$  is independent and identically distributed (i.i.d.) random variables with  $\mathcal{CN}(0, 1)$  distribution, i.e., Rayleigh fading channels. Similarly, the channel of the second link is modeled as  $h_{rd} = \sqrt{\rho_{rd}}\bar{h}_{rd}$ , where  $\rho_{rd}$  is the large-scale fading between RN and DN and  $\bar{h}_{rd} \sim \mathcal{CN}(0, 1)$  is the small-scale fading.

At time  $t$ , instantaneous achievable rates of the first and second links are written as follows.

$$R_s(t) = \frac{1}{2} \log_2 (1 + \gamma_{sr}(t)) = \frac{1}{2} \log_2 \left( 1 + \frac{P_s \rho_{sr} |h_{sr}(t)|^2}{\sigma_r^2} \right), \quad (1)$$

$$R_r(t) = \frac{1}{2} \log_2 (1 + \gamma_{rd}(t)) = \frac{1}{2} \log_2 \left( 1 + \frac{P_r \rho_{rd} |h_{rd}(t)|^2}{\sigma_d^2} \right), \quad (2)$$

where  $\gamma_{sr}(t)$  and  $\gamma_{rd}(t)$  are the instantaneous signal-to-noise ratios (SNRs) at RN and DN, respectively;  $P_s$  and  $P_r$  are the transmit power of SN and RN, respectively; and  $\sigma_r^2$  and  $\sigma_d^2$  are the variances of the additive white Gaussian noise (AWGN) at the RN and DN, respectively; without loss of generality, the average power of the symbols transmitted from SN and RN is assumed to be one.

When the first link is better than the second link, i.e.,  $\gamma_{sr} \geq \gamma_{rd}$  and equivalently  $R_r(t) \geq R_s(t)$ , no matter how much information is delivered from SN to RN, the RN can forward no greater than  $R_r(t)$ . On the other hand, even if  $\rho_{sr} < \rho_{rd}$ , the RN cannot forward more information than what RN received, i.e., information causality [1,21]. Thus, the instantaneous achievable rate of the overall link at time  $t$  is written as follows [2,3]:

$$R(t) = \min\{R_s(t), R_r(t)\}. \quad (3)$$

Using (3), the average achievable rate for  $T$  seconds is obtained as

$$R(P_r) = \frac{1}{T} \sum_{t=1}^T R(t), \quad (4)$$

where note that the average achievable rate is a function of the transmit power of RN, i.e.,  $P_r$ , which will be designed later.

## 3. Achievable Rate of RN with a Buffer

An RN employs a buffer that can reserve the information bits. The buffered bits are received from SN, yet not forwarded to DN if the channel condition of the second link is poor. The bits in the buffer are forwarded later once the channel condition changes to be good. Considering the limited buffer size,  $b$ , and information causality, we can consider two cases as follows.

- $R_s(t) \geq R_r(t)$ : RN forwards  $R_r(t)$  and reserves the remaining bits, i.e.,  $R_s(t) - R_r(t)$  bits, at the buffer unless the buffer is full with  $b$  bits. Thus, the buffer status at time  $t$  will be  $\min(B(t-1) + (R_s(t) - R_r(t)), b)$ , where  $B(0) = 0$ .
- $R_s(t) < R_r(t)$ : RN forwards  $R_s(t)$ . In this case, since RN can forward more bits up to  $R_r(t) - R_s(t)$ , the number of forwarded bits will be  $R_s(t) + \min(B(t-1), R_r(t) - R_s(t))$ . Accordingly, the buffer status will be  $\max(B(t-1) - (R_r(t) - R_s(t)), 0)$ .

Concretely, by virtue of the buffer, the achievable rate of the overall link with the buffer-aided RN and the buffer status at time  $t$  are written as follows.

$$R_B(t) = \begin{cases} R_r(t), & \text{if } R_s(t) \geq R_r(t) \\ R_s(t) + \min(B(t-1), R_r(t) - R_s(t)), & \text{otherwise} \end{cases} \quad (5)$$

$$B(t) = \begin{cases} \min(B(t-1) + (R_s(t) - R_r(t)), b), & \text{if } R_s(t) \geq R_r(t) \\ \max(B(t-1) - (R_r(t) - R_s(t)), 0), & \text{otherwise} \end{cases} \quad (6)$$

For example, Figure 2 shows the status of a buffer with  $b = 2$  for  $T = 500$  when  $\gamma_{sr} = 10$  dB. From the results, it is clearly observed that the buffer operates as expected. When the first link is better than the second link, i.e.,  $\gamma_{sr} \gg \gamma_{rd}$ , the information amount delivered from SN to RN is greater than that forwarded from RN to DN. Thus, the buffer is almost always full when  $\gamma_{rd} = 0$  dB, as shown in Figure 2a. On the other hand, as  $\gamma_{rd}$  increases to 10 dB and 20 dB, the information amount forwarded from RN to DN increases, resulting in the reduction of information bits in the buffer as shown in Figure 2b,c, respectively. When  $\gamma_{rd} = 30$  dB, the buffer is almost empty as shown in Figure 2d. Here, we propose that the size of the buffer is critical for the achievable rate of the RN networks.

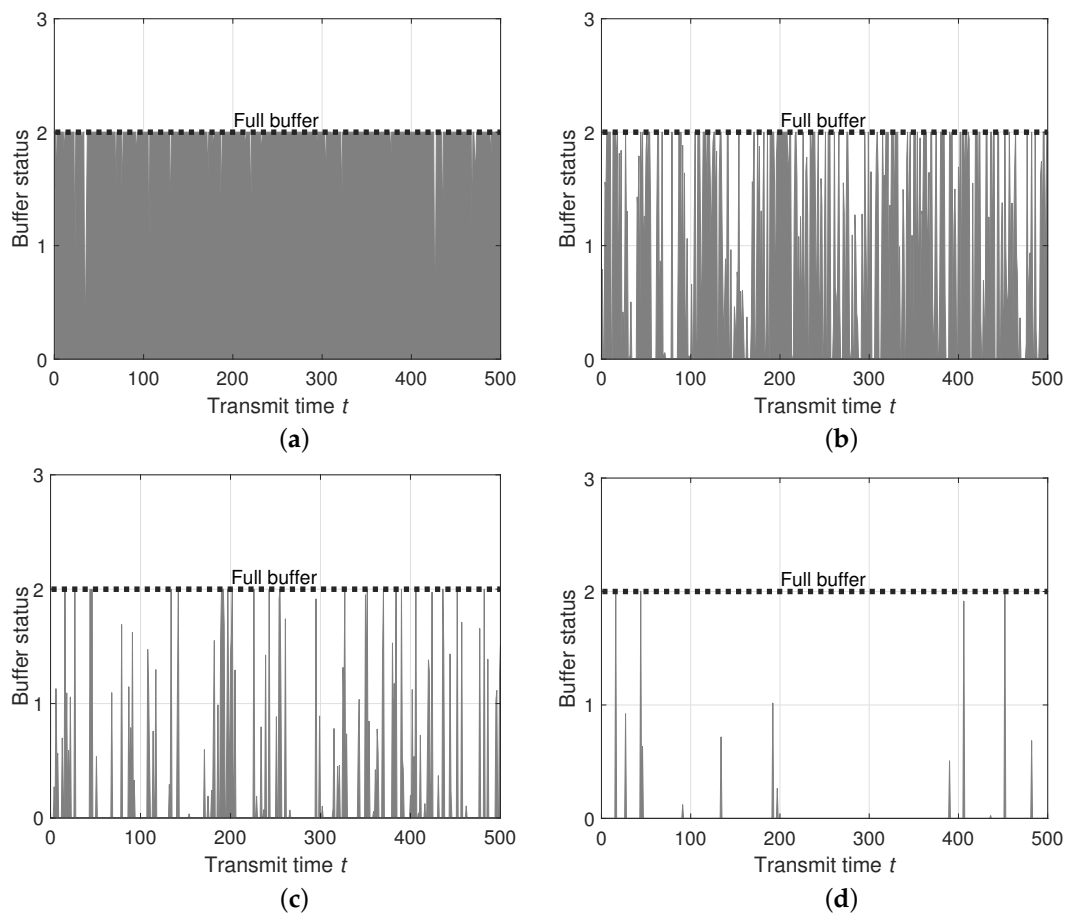


**Figure 2.** Buffer status when  $\gamma_{sr} = 10$  dB and buffer size is two bits, i.e.,  $b = 2$ . (a)  $\gamma_{rd} = 0$  dB. (b)  $\gamma_{rd} = 10$  dB. (c)  $\gamma_{rd} = 15$  dB. (d)  $\gamma_{rd} = 25$  dB.

#### 4. Buffer Size Design

To determine an efficient buffer size, we evaluate the average achievable rate of  $R_B(t)$  in Equation (5), which is defined as

$$R_B(P_r) = \frac{1}{T} \sum_{t=1}^T R_B(t). \quad (7)$$

Figure 3 shows the average achievable rates in Equations (4) and (7) by varying the buffer size  $b$  when  $\gamma_{sr} = 20$  dB. Data transmission time is given as  $T = 10^5$ . Obviously, the relay system without a buffer is a special case of the relay system with a buffer whose size is zero, i.e.,  $b = 0$ . By comparing the rates at  $b = 0$  and  $b > 0$ , it is clearly observed that the buffer can improve the achievable rate of the cooperative systems. It is also observed that the achievable rate increases and it is saturated as buffer size  $b$  increases. As observed in the results, the average achievable rate is almost saturated when the buffer size  $b = 10$ , regardless of  $\gamma_{rd}$ . From the results, the size of an effective buffer is determined by ten for the considered relay system in this study.

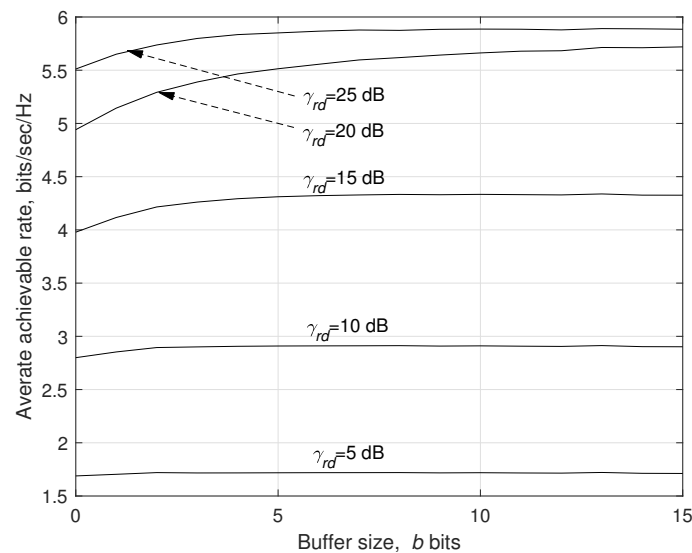


**Figure 3.** Average achievable rate  $R_B$  in Equation (7) over the buffer size  $b$  bits when  $\gamma_{sd} = 20$  dB.

Now, to justify that the proposed buffer-aided relay system with  $b = 10$  outperforms the conventional relay system without a buffer, the average achievable rates  $R(P_r)$  and  $R_B(P_r)$  defined in Equations (4) and (7), respectively, are evaluated over the transmit power of RN, i.e.,  $P_r$ .

In Figure 4,  $R(P_r)$  in Equation (4) and  $R_B(P_r)$  in Equation (7) are compared across  $P_r$ . In simulation, it is assumed that the channel attenuation follows the model in works by the authors of [31–34] as follows

$$\rho_A = G - 128 + 10 \log_{10}(d_A^{-\alpha}) \text{ dB}, \quad (8)$$

where  $A \in \{sr, rd\}$ ,  $G$  includes the transceiver feeder loss and antenna gains,  $d_A^{-\alpha}$  is the path loss where  $d_A$  is the distance in kilometer between nodes, and  $\alpha$  is a path loss exponent. The transmit power of SN is fixed as  $P_s = 23$  dBm. In model (8), we set  $G = 5$  dB (2 dB and 0 dB feeder losses at the transmitter and receiver, respectively; and 7 dBi and 0 dBi gains for the transmit and receive antennas, respectively [31]),  $\alpha = 3.76$  (for urban or suburban environment [35]),  $\sigma_r^2 = \sigma_d^2 = -174$  dBm/Hz for AWGN power [31], and  $P_s = 23$  dBm for small-size BS [34]. On the other hand, the transmit power of RN varies between 17 dBm and 33 dBm (note that 33 dBm, 21 dBm, and 17 dBm for the transmit power of micro, pico, and femto BSs, respectively [34]). The distance between GBS and RN is set as  $d_{sr} = 0.6$  km.

From the results, it is clearly shown that  $R_B(P_r) \geq R(P_r)$ . For given  $P_s$ , the average data rate increases up to a certain point and is saturated as  $P_r$  increases. The saturation point of  $P_r$  of the buffer-aided relay is lower than that of the relay without a buffer. From this, it is verified that the buffer-aided relay system efficiently utilizes the second-link channel in virtue of opportunistic forwarding; therefore, the greater average achievable rate is achieved. Thus, from this fact, the transmit power of RN can be reduced sustaining the throughput such that it is identical to the throughput without a buffer, i.e.,  $R_B(P_r^o) = R(P_r)$ , where  $P_r^o < P_r$ . Consequently, it is expected that EE of the network can be improved.

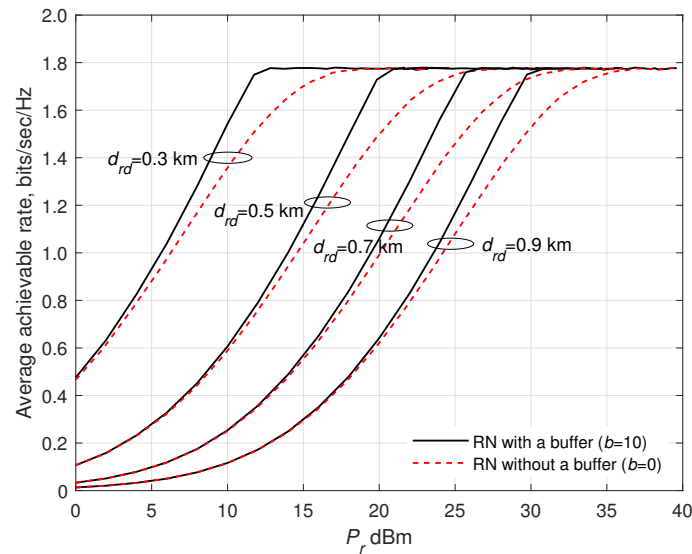


Figure 4. Average achievable rate when  $P_s = 23$  dBm,  $b = 10$ , and  $d_{sr} = 0.6$  km.

### 5. Proposed Power Control Method for Energy Efficient RN

The EE of the network with respect to RN is defined as a ratio of the average achievable rate and the power consumption at RN as follows [32–34,36–38].

$$EE(P_r) = \frac{R_B(P_r)}{\eta P_r + P_c'} \quad (9)$$

where  $\eta$  represents system inefficiency ( $\eta > 1$ ) that is caused by overhead power consumption at radio frequency circuits, and  $P_c$  is the power consumption which is independent of transmit power. The first term in the denominator of Equation (9) is thus the power consumption at the power amplifier of RN. On the other hand, the second term in the denominator of Equation (9) includes a part of power consumption for communication at, for example, a power supply, an alternating current to direct current (AC/DC) converter, a DC/DC converter, and an active cooling system, and the propulsion power consumption for hovering [39].

To design  $P_r$ , such that EE in Equation (9) is maximized, we evaluate the EE over  $P_r$ . In Figure 5, the EEs of two relay systems with and without a 10-bit buffer are compared when  $P_s = 23$  dBm,  $d_{sr} = 0.6$  km, and  $d_{rd} \in \{0.3, 0.6, 0.9\}$ . For the power consumption parameters, we set them as  $\eta = 5.26$  and  $P_c \in \{10, 20, 30, 40\}$  dBm. Here, the values of simulation parameter are typical for the wireless communication systems (refer to works by the authors of [32–34,36–38] and references therein), and they can be adjusted according to the application systems. Note the the proposed power control framework, which is introduced shortly, is independent of the values of parameters. From the results in Figure 5, we can verify that the EE can be improved by using a buffer at RN, regardless of  $d_{rd}$  and  $P_c$ .

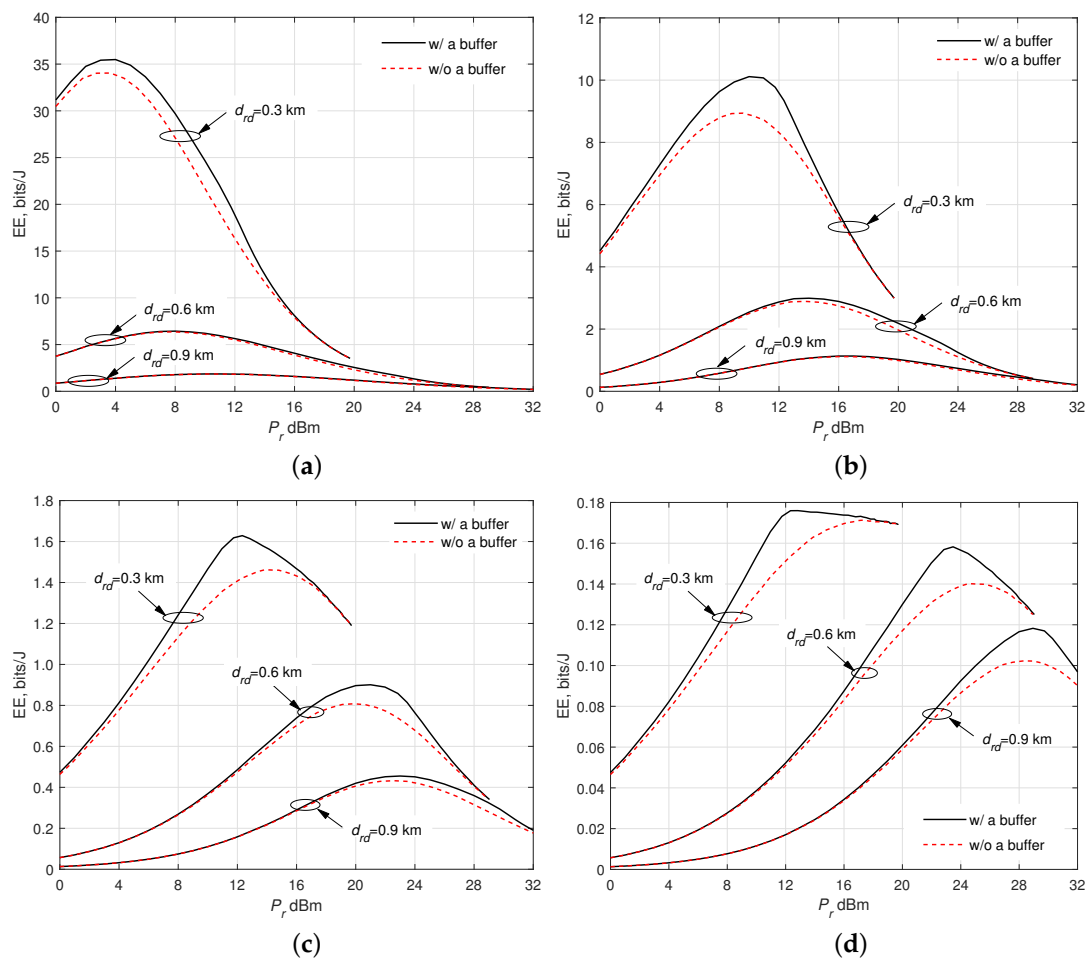


**Figure 5.** EE across  $P_r$  when  $P_s = 23$  dBm,  $d_{sr} = 0.6$  km,  $d_{rd} \in \{0.3, 0.6, 0.9\}$  km, and  $\eta = 5.26$ . (a)  $P_c = 10$  dBm. (b)  $P_c = 20$  dBm. (c)  $P_c = 30$  dBm. (d)  $P_c = 40$  dBm.

It is also observed from Figure 5 that the EE function is a unimodal function having a unique maximum of EE. However, to analytically find the optimal  $P_r$  maximizing EE is challenging. Using Equations (1), (5), and (7)–(9), we see that the EE function is intractable, i.e., there is no closed form of the first derivative of EE with respect to  $P_r$ . One can immediately consider a one-dimensional numerical search algorithms, such as golden section search, quadratic interpolation method, and inexact line searches, to find the local optimal solution [40], or machine learning based algorithm, e.g., reinforcement learning [41–43]. However, since the average achievable rate needs to be fed back from DN to RN for each iteration with adapted  $P_r$  to estimate the EE, the iterative approaches require significant overhead of the networks. In the work by the authors of [24], the EE is analytically maximized by optimally allocating the frequency and transmit power resources. To this end, however, the transmitter, namely SN and RN, should know the channel state information among the nodes. Though the analytical approach can provide the optimal EE performance, this analytical strategy is challenging to be practically implemented, due to the network overhead. Thus, in this study, we employ a two-dimensional surface fitting method to model the optimal transmit power of RN as a function of two essential variables of EE, namely  $d_{rd}$  and  $P_c$ .

In Figure 6, the optimal  $P_r^o$ 's are shown for  $d_{rd} \in \{0.3, 0.6, 0.9\}$  and  $P_c \in \{10, 20, 40, 40\}$ , which are obtained from Figure 5. The optimal transmit power of RN, i.e.,  $P_r^o$  increases as  $P_c$  or  $d_{rd}$  increases. To fit the optimal points of  $P_r^o$  to a surface, the multidimensional regression methods are employed [44]. In this study, we employ a polynomial surface fitting method, which is simple to design based on the

least squares method and requires a small amount of memory at the RN. The quadratic polynomial surface is modeled as follows.

$$P_r(d_{rd}, P_c) = -8.462 + 27.89d_{rd} + 0.5436P_c - 21.9d_{rd}^2 + 0.5985d_{rd}P_c - 0.008475P_c^2 \quad (10)$$

and it is shown in Figure 7. Similarly, for the optimal points,  $P_r^o$ 's of RN without a buffer in Figure 6 can be modeled as a surface. The quadratic polynomial surface of  $P_r^o$  of RN without a buffer can be modeled as

$$P_r(d_{rd}, P_c) = -8.12 + 25.1d_{rd} + 0.5353P_c - 15.29d_{rd}^2 + 0.2674d_{rd}P_c - 0.003055P_c^2. \quad (11)$$

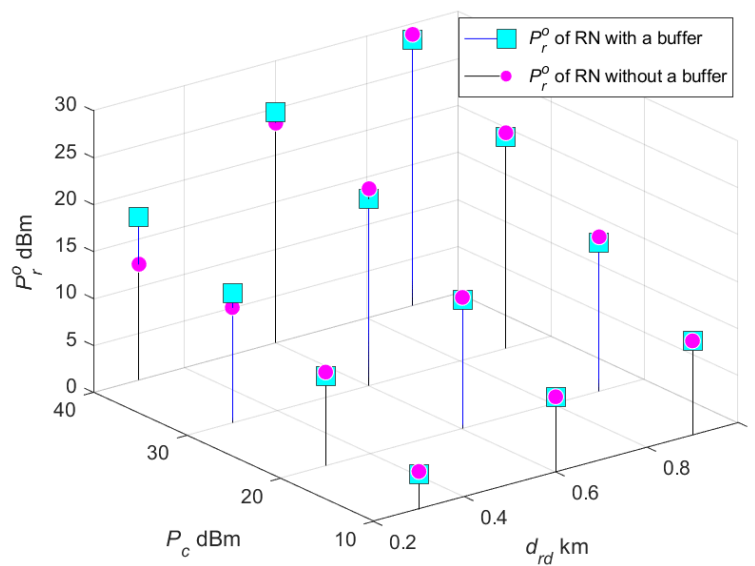


Figure 6. Optimal power  $P_r^o$  of RN with and without a buffer over  $d_{rd}$  and  $P_c$ , where  $P_r^o$  is obtained from the results in Figure 5.

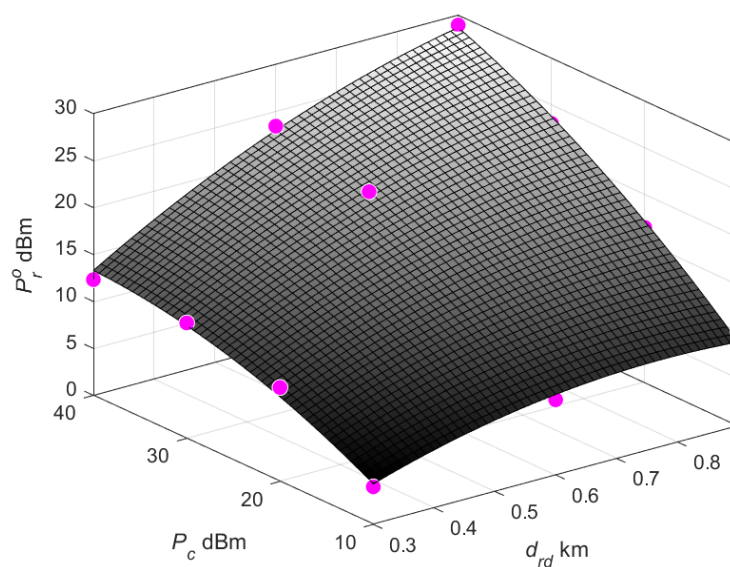


Figure 7. Surface fitted from  $P_r^o$  with a buffer in Figure 6 by using a polynomial surface fitting method.



Using Equations (10) and (11), the RN can determine its transmit power  $P_r$  if it knows  $P_c$  and  $d_{rd}$ . Here, it is worth noting that  $P_c$  is local information, which can be readily measured at the RN, and that the distance  $d_{rd}$  can also be measured at the RN based on the received signal strength from DN. Therefore, the proposed RN power control method can be easily implementable at the RN. For the applications of discrete-level power control, the quantized output of the quadratic polynomial surfaces in Equations (10) and (11) can be used. In this study, we leave the measurement or prediction method for  $P_c$  and  $d_{rd}$  as future work. In the next section, the proposed RN power control methods using Equations (10) and (11) are verified by evaluating the EE performance.

## 6. Numerical Results and Discussion

In this section, EE is evaluated by varying  $P_c$  and  $d_{rd}$ . We compare five power control (PC) schemes:

- EE-based PC w/ a buffer: The proposed RN system with a buffer. The RN transmit power is controlled by a one-dimensional numerical search. This method can be interpreted as a numerical approach of the optimal strategy in the work by the authors of [24], for a single pair of RN and DN. This is optimal yet impractical approach as stated in the previous section.
- EE-based PC w/ a buffer: The proposed RN system with a buffer. The RN transmit power is controlled by Equation (10).
- EE-based PC w/o a buffer: The conventional RN system without a buffer. The RN transmit power is controlled by Equation (11). The PC method is designed in this study, yet it is employed to the conventional RN for the sake of comparison. This method can be interpreted as an EE-based power control method in [18].
- SE-based PC w/ a buffer: PC is performed to maximize SE [2,3]. Here, the RN employs a buffer.
- SE-based PC w/o a buffer: PC is performed to maximize SE [2,3]. Here, the RN does not employ a buffer.

In Figure 8, each subfigure shows EE by varying  $P_c$  for fixed  $d_{rd}$ . From the results, the proposed PC is verified that it can achieve the near-optimal EE regardless of the power consumption model, i.e.,  $P_c$ , and the distance  $d_{rd}$ . Clearly, EE decreases as  $P_c$  increases. It is also observed that the proposed PC can also significantly improve EE for the relay system without a buffer. On the other hand, SE-based PC methods do not provide comparable EE to the relay system with EE-based PC. Here, note that the transmit power of RN of SE-based PC methods is fixed as it is independent of the power consumption model. The fixed parameters of power are as follows:  $P_r = 13$  dBm and  $P_r = 20$  dBm for RN with and without a buffer, respectively, when  $d_{rd} = 0.3$  km in Figure 8a;  $P_r = 22$  dBm and  $P_r = 30$  dBm for RN with and without a buffer, respectively, when  $d_{rd} = 0.5$  km in Figure 8b;  $P_r = 27$  dBm and  $P_r = 35$  dBm for RN with and without a buffer, respectively, when  $d_{rd} = 0.7$  km in Figure 8c; and  $P_r = 32$  dBm and  $P_r = 40$  dBm for RN with and without a buffer, respectively, when  $d_{rd} = 0.9$  km in Figure 8d. This is because, as previously shown in Figure 6, the transmit power of RN is needed to increase to improve EE as  $P_c$  or  $d_{rd}$  increases. The SE-based fixed PC may achieve the best EE, e.g., when  $P_c$  is high. However, the fixed PC strategies are inefficient since  $P_c$  may vary in time due to the external environment variation, such as temperature and humidity. Moreover, even  $P_c$  is fixed,  $d_{rd}$  may vary and accordingly the optimal  $P_r$  also varies. To clarify it, the next simulation is performed for fixed  $P_c$  by varying  $d_{rd}$ .

In Figure 9, each subfigure shows EE by varying  $d_{rd}$  for fixed  $P_c$ . Clearly, EE decreases as  $d_{rd}$  increases. The proposed PC can achieve the near-optimal EE regardless of the power consumption model, i.e.,  $P_c$ , and the distance  $d_{rd}$ . It is also observed that the proposed EE-based PC can also improve EE for the RN system without a buffer, especially, when  $P_c$  is small. However, the EE gap between RN with and without a buffer increases as  $P_c$  increases. From this results, we see that the buffer is more efficient when  $P_c$  is large. Though the SE-based PC methods optimize  $P_r$  according to  $d_{rd}$ , their EE performance is not comparable to the EE of the proposed EE-based PC methods for RN with a

buffer. As expected, the proposed RN system with a buffer and PC is superior to others regardless of  $P_c$  and  $d_{rd}$ .

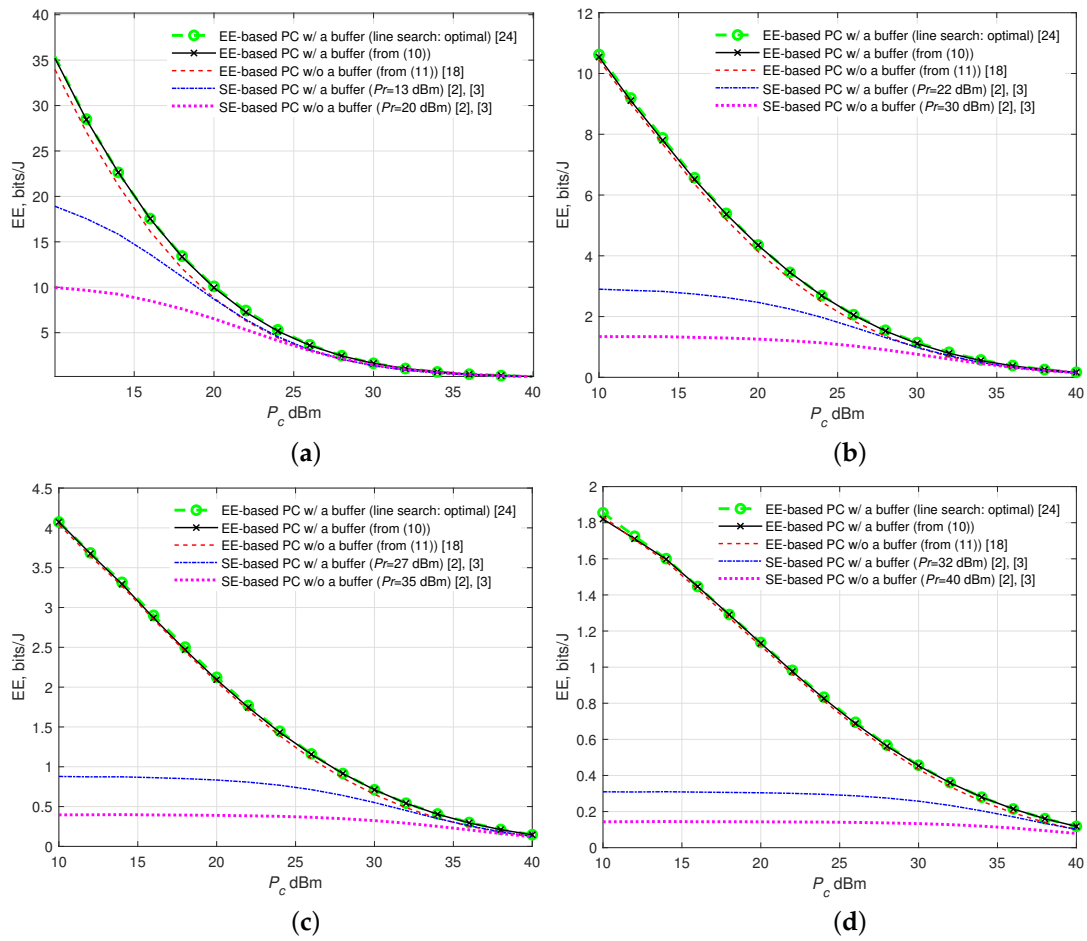


**Figure 8.** EE across  $P_c$  with EE- and SE-based power control (PC) for RN. (a)  $d_{rd} = 0.3$  km. (b)  $d_{rd} = 0.5$  km. (c)  $d_{rd} = 0.7$  km. (d)  $d_{rd} = 0.9$  km.

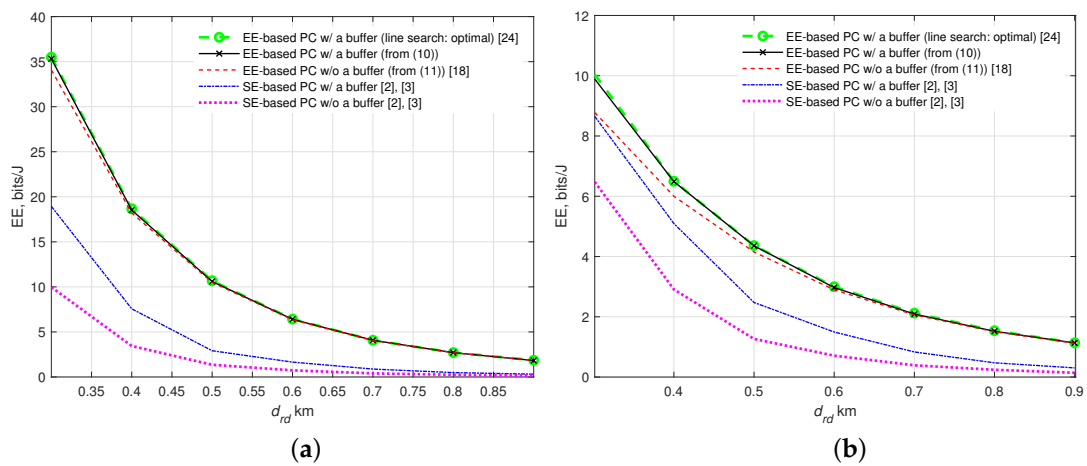


**Figure 9.** Cont.

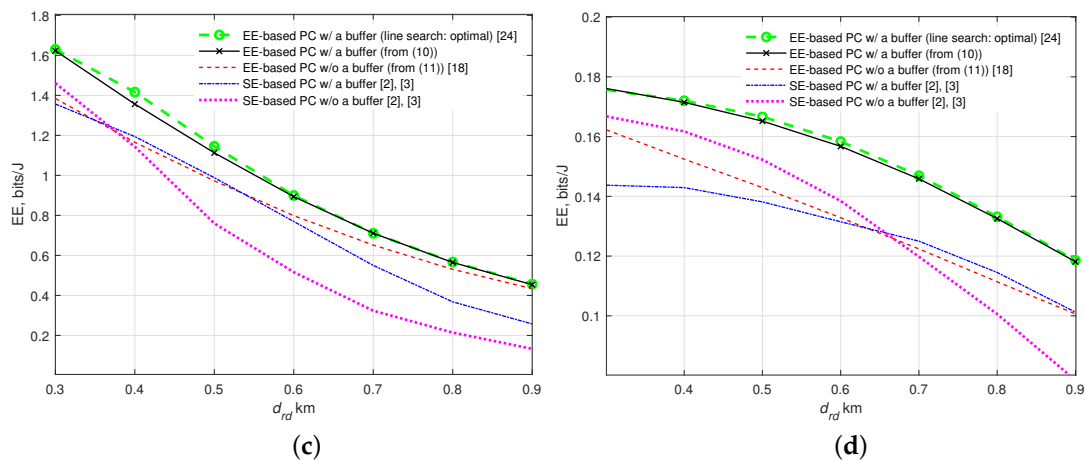


**Figure 9.** EE across  $d_{rd}$  for RN with a power control (PC) for RN. (a)  $P_c = 10$  dBm. (b)  $P_c = 20$  dBm. (c)  $P_c = 30$  dBm. (d)  $P_c = 40$  dBm.

## 7. Conclusions

In this study, a relay system has been considered, in which a ground source node (SN) sends information to a destination node (DN) through an unmanned aerial vehicle relay node (RN) with a buffer. When the transmit power of SN is fixed, we have proposed a two-dimensional surface fitting method to simply obtain the near-optimal transmit power of RN to maximize the energy efficiency (EE) of the RN. To this end, the RN needs its power consumption model and the distance from a DN. From the rigorous numerical results, it has been verified that the proposed power control method can significantly improve the EE of RN compared to a fixed power control method based on spectral efficiency, and achieve near-optimal performance.

**Author Contributions:** Conceptualization, J.J. and H.L.L.; methodology, J.J.; software, J.Z.; validation, J.Z and X.K.; investigation, J.Z.; writing, original draft preparation, J.J.; review and editing, H.L.L, J.Z. and X.K.; visualization, J.J. and H.L.L.; supervision, J.J.; project administration, J.J.; funding acquisition, J.J.

**Funding:** This research was supported by the National Research Foundation of Korea (NRF) grant (2018R1A4A1023826) funded by the Korean government (MSIT).

**Conflicts of Interest:** The authors declare no conflicts of interest.

## References

- Cover, T.M.; El Gammal, A. Capacity theorems for relay channels. *IEEE Trans. Inf. Theory* **1979**, *25*, 572–584. [[CrossRef](#)]
- Rankov, B.; Wittneben, A. Spectral efficient protocols for half-duplex fading relay channels. *IEEE J. Sel. Areas Commun.* **2007**, *25*, 379–389. [[CrossRef](#)]
- Zhao, J.; Kuhn, M.; Wittneben, A.; Bauch, G. Cooperative transmission schemes for decode-and-forward relaying. In Proceedings of the 2007 IEEE 18th International Symposium on Personal, Indoor and Mobile Radio Communications, Athens, Greece, 3–7 September 2007; pp. 1–5.
- Darsena, D.; Gelli, G.; Iudice, I.; Verde, F. Widely-linear transceiver design for amplify-and-forward MIMO relaying. In Proceedings of the 2016 IEEE Sensor Array and Multichannel Signal Processing Workshop (SAM), Rio de Janeiro, Brazil, 10–13 July 2016; pp. 1–5.
- Barman Roy, S.; Madhukumar, A.S.; Joung, J. On joint Pareto frontier in multiple access and relay rate regions with Rayleigh fading. *IEEE Trans. Veh. Technol.* **2017**, *66*, 3777–3786.
- Joung, J.; Sayed, A.H. Multiuser two-way amplify-and-forward relay processing and power control methods for beamforming systems. *IEEE Trans. Signal Process.* **2010**, *58*, 1833–1846. [[CrossRef](#)]
- Joung, J.; Sayed, A.H. User selection methods for multiuser two-way relay communications using space division multiple access. *IEEE Trans. Wirel. Commun.* **2010**, *9*, 2130–2136. [[CrossRef](#)]

8. Patel, C.S.; Stuber, G.L. Channel estimation for amplify and forward relay based cooperation diversity systems. *IEEE Trans. Wirel. Commun.* **2007**, *6*, 2348–2356. [[CrossRef](#)]
9. Unger, T.; Klein, A. Applying relay stations with multiple antennas in the one- and two-way relay channel. In Proceedings of the IEEE 18th International Symposium on Personal, Indoor and Mobile Radio Communications, (PIMRC), Athens, Greece, 3–7 September 2007.
10. Chun, B.; Jeong, E.R.; Joung, J.; Oh, Y.; Lee, Y.H. Pre-nulling for self-interference suppression in full-duplex relays. In Proceedings of the 2009 APSIPA Annual Summit and Conference, Sapporo, Japan, 4–7 October 2009; pp. 949–952.
11. Joung, J.; Sun, S. Design and performance evaluation of multiple AF-relay processing in multi-cell environment. In Proceedings of the 2011 IEEE 73rd Vehicular Technology Conference (VTC Spring), Budapest, Hungary, 15–18 May 2011; pp. 1–5.
12. Joung, J.; Sun, S. A simple network-power-saving resource allocation method for OFDMA cellular networks with multiple relays. In Proceedings of the 2011 IEEE International Conference on Acoustics, Speech and Signal Processing (ICASSP), Prague, Czech Republic, 22–27 May 2011; pp. 2504–2507.
13. Hammerström, I.; Kuhn, M.; Ešli, C.; Zhao, J.; Wittneben, A.; Bauch, G. MIMO two-way relaying with transmit CSI at the relay. In Proceedings of the IEEE Signal Processing Advances in Wireless Communications (SPAWC), Helsinki, Finland, 17–20 June 2007.
14. Ye, H.T.; Kang, X.; Liang, Y.C.; Joung, J. Full-duplex wireless-powered IoT networks with unmanned aerial vehicle. In Proceedings of the The 9th International Conf. ICT Convergence (ICTC), Jeju Island, Korea, 17–19 October 2018; pp. 1–4.
15. Zhang, S.; Zhang, H.; He, Q.; Bian, K.; Song, L. Joint trajectory and power optimization for UAV relay networks. *IEEE Commun. Lett.* **2018**, *22*, 161–164. [[CrossRef](#)]
16. Ye, H.T.; Kang, X.; Liang, Y.C.; Joung, J. Optimal time allocation for full-duplex wireless-powered IoT networks with unmanned aerial vehicle. In Proceedings of the IEEE International Conference on Communications (ICC), Shanghai, China, 20–24 May 2019; pp. 1–6.
17. Kang, H.; Joung, J.; Ahn, J.; Kang, J. Secrecy-aware altitude optimization for quasistatic UAV base station without eavesdropper location information. *IEEE Commun. Lett.* **2019**, *23*, 851–854. [[CrossRef](#)]
18. Joung, J.; Sun, S. Power efficient resource allocation for downlink OFDMA relay cellular networks. *IEEE Trans. Signal Process.* **2012**, *60*, 2447–2459. [[CrossRef](#)]
19. Singh, K.; Ku, M.L.; Biswas, S.; Ratnarajah, T. Energy-efficient subcarrier pairing and power allocation for DF relay networks with an eavesdropper. *Energies* **2017**, *10*, 1953. [[CrossRef](#)]
20. Zhang, J.; Zeng, Y.; Zhang, R. Spectrum and energy efficiency maximization in UAV-enabled mobile relaying. In Proceedings of the IEEE International Conference on Communications (ICC), Paris, France, 21–25 May 2017; pp. 1–6.
21. Xia, B.; Fan, Y.; Thompson, J.; Poor, H.V. Buffering in a three-node relay network. *IEEE Trans. Wirel. Commun.* **2008**, *7*, 4492–4496. [[CrossRef](#)]
22. Zlatanov, N.; Schober, R. Buffer-aided relaying with adaptive link selection-fixed and mixed rate transmission. *IEEE Trans. Inf. Theory* **2013**, *59*, 2816–28404. [[CrossRef](#)]
23. Qiao, D. Effective capacity of buffer-aided full-duplex relay systems with selection relaying. *IEEE Trans. Veh. Technol.* **2016**, *64*, 117–129. [[CrossRef](#)]
24. Hajipour, J.; Niya, J.M.; Ng, D.W.K. Energy-efficient resource allocation in buffer-aided wireless relay networks. *IEEE Trans. Wirel. Commun.* **2017**, *16*, 6648–6659. [[CrossRef](#)]
25. Nakai, R.; Oiwa, M.; Sugiura, S. Generalized buffer-state-based relay selection for fixed-rate buffer-aided cooperative systems. In Proceedings of the IEEE 85th Vehicular Technology Conference (VTC Spring), Sydney, NSW, Australia, 4–7 June 2017; pp. 1–5.
26. Haneda, K.; Kahra, E.; Wyne, S.; Icheln, C.; Vainikainen, P. Measurement of loop-back interference channels for outdoor-to-indoor full-duplex radio relays. In Proceedings of the Fourth European Conference Antennas and Propagation, Barcelona, Spain, 12–16 April 2010; pp. 1–5.
27. Cumanan, K.; Ding, Z.; Rahulamathavan, Y.; Molu, M.M.; Chen, H. Robust MMSE beamforming for multiantenna relay networks. *IEEE Trans. Veh. Technol.* **2017**, *66*, 3900–3912. [[CrossRef](#)]
28. Joung, J.; Sun, S. Phase rotation and link selection methods for DFTTD-based two-path relay systems. *IEEE Commun. Lett.* **2011**, *15*, 278–280. [[CrossRef](#)]

29. Joung, J. Beamforming vector design for regenerative wired two-way relay systems. *IET Electron. Lett.* **2017**, *53*, 596–598. [CrossRef]
30. Joung, J.; Choi, J. Linear precoder design for an AF two-way MIMO relay node with no source node precoding. *IEEE Trans. Veh. Technol.* **2017**, *66*, 10526–10531. [CrossRef]
31. LTE; E-UTRA. RF Requirements for LTE Pico Node B; ETSI std., 136 931 V9.0.0; 2011. Available online: [https://www.etsi.org/deliver/etsi\\_tr/136900\\_136999/136931/09.00.00\\_60/tr\\_136931v090000p.pdf](https://www.etsi.org/deliver/etsi_tr/136900_136999/136931/09.00.00_60/tr_136931v090000p.pdf) (accessed on 22 August 2019).
32. Joung, J.; Sun, S. Energy efficient power control for distributed transmitters with ZF-based multiuser MIMO precoding. *IEEE Commun. Lett.* **2013**, *17*, 1766–1769. [CrossRef]
33. Joung, J.; Chia, Y.K.; Sun, S. Energy-efficient, large-scale distributed-antenna system (L-DAS) for multiple users. *IEEE J. Sel. Topics Signal Process.* **2014**, *8*, 954–965. [CrossRef]
34. Joung, J.; Ho, C.K.; Sun, S. Spectral efficiency and energy efficiency of OFDM systems: Impact of power amplifiers and countermeasures. *IEEE J. Sel. Areas Commun.* **2014**, *32*, 208–220, doi:10.1109/JSAC.2014.141203. [CrossRef]
35. Rappaport, T.S. *Wireless Communications*, 2nd ed.; Prentice Hall: Upper Saddle River, NJ, USA, 2002.
36. Joung, J.; Ho, C.K.; Sun, S. Power amplifier switching (PAS) for energy efficient systems. *IEEE Wirel. Commun. Lett.* **2013**, *2*, 14–17. [CrossRef]
37. Joung, J.; Sun, S. EMA: Energy-efficiency-aware multiple access. *IEEE Commun. Lett.* **2014**, *18*, 1071–1074. [CrossRef]
38. Joung, J.; Ho, C.K.; Adachi, K.; Sun, S. A survey on power-amplifier-centric techniques for spectrum and energy efficient wireless communications. *IEEE Commun. Surv. Tutor.* **2014**, *17*, 315–333. [CrossRef]
39. Zeng, Y.; Xu, J.; Zhang, R. Energy minimization for wireless communication with rotary-wing UAV. *IEEE Trans. Wirel. Commun.* **2019**, *18*, 2329–2345. [CrossRef]
40. Antoniou, A.; Lu, W.S. *Practical Optimization: Algorithms and Engineering Applications*, 1st ed.; Springer: New York, NY, USA, 2007.
41. Joung, J. Machine learning-based antenna selection in wireless communications. *IEEE Commun. Lett.* **2016**, *20*, 2241–2244. [CrossRef]
42. Jadoon, M.A.; Kim, S. Relay selection algorithm for wireless cooperative networks: A learning-based approach. *IET Commun.* **2017**, *11*, 1061–1066. [CrossRef]
43. Abdelreheem, A.; Omer, O.A.; Esmail, H.; Mohamed, U.S. Deep learning-based relay selection in D2D millimeter wave communications. In Proceedings of the 2019 International Conference on Computer and Information Sciences (ICCIS), Milan, Italy, 30 October–1 November 2019; pp. 1–5.
44. Chapra, S.C. *Applied Numerical Methods with MATLAB for Engineers and Scientists*, 3rd ed.; Mc Graw Hill: Singapore, 2012.



© 2019 by the authors. Licensee MDPI, Basel, Switzerland. This article is an open access article distributed under the terms and conditions of the Creative Commons Attribution (CC BY) license (<http://creativecommons.org/licenses/by/4.0/>).